Journal of the European Ceramic Society **5** (1989) 311–319

Sintering of Si_3N_4 with Y_2O_3 and Al_2O_3 Added by Coprecipitation

Ji-Soon Kim, Helmut Schubert & Günter Petzow

Max-Planck-Institut für Metallforschung, Institut für Werkstoffwissenschaft, Pulvermetallurgisches Laboratorium, 7000 Stuttgart 80, FRG

(Received 29 August 1989; accepted 5 December 1989)

Abstract

The aim of this work was to improve the chemical and geometrical homogeneity of Si_3N_4 powder by applying wet chemical preparation routes for the dispersion of sintering additives in Si_3N_4. The conventional Y_2O_3–Al_2O_3 additive system with 3:5 molar ratio (YAG) has been chosen as a standard composition. The amount added was 5, 10 and 15 mole%, respectively. Three routes have been comparably tested: precipitation of hydroxides from nitrates with ammonia onto the Si_3N_4 surfaces, precipitation in the absence of Si_3N_4 followed by mechanical mixing with Si_3N_4, and mechanical mixing of oxides with Si_3N_4 in an attrition mill.

The calcination of the powders was found to be a critical preparation step due to the risk of picking-up of additional oxygen, which results in the Si_2N_2O formation and slows down the densification. For calcination at 900°C under N_2, the sintering behavior of the precipitated powder was favorable and 2·7% higher final density could be achieved for identical sintering parameters.

Das Ziel dieser Arbeit war die Verbesserung der chemischen und geometrischen Homogenität von Si_3N_4-Pulvern durch die Anwendung von naßchemischen Verfahren zur Verteilung der Sinteradditive im Si_3N_4-Pulver.

Als Additive wurde das konventionelle Y_2O_3–Al_2O_3-System mit einem molaren Verhältnis von 3:5 (YAG) gewählt. Es wurden 5, 10 und 15 mol-% beigegeben und 3 verschiedene Verfahrenswege im Vergleich getestet: Die direkte Präzipitation der Hydroxide aus Nitratverbindungen in Ammoniak auf die Siliziumnitridoberflächen, die separate Fällung der Hydroxide, gefolgt von einem mechanischen Mischen von Additiv und Si_3N_4 und die mechanische Mischung der Oxide mit Si_3N_4 in einem Attritor.

Die Kalzination der Pulver war ein kritischer Schritt in dem Herstellungsprozeß, weil die Gefahr der Sauerstoffaufnahme bestind, die zur Bildung von Si_2N_2O führe und die Verdichtung verringert. Wenn die Kalzination in Stickstoff bei 900°C durchgeführt wurde, war das Sinterverhalten der präzipitierten Pulver gut und es konnte unter den gleichen Sinterbedingungen eine um 2·7% höhere Enddichte erreicht werden.

Le but de cette étude était d'améliorer l'homogénéité chimique et géométrique d'une poudre de Si_3N_4 en dispersant les additifs de frittage synthétisés par voie chimique en solution. L'additif classique du système Y_2O_3–Al_2O_3 de rapport molaire 3:5 (YAG) a été choisi. Les quantités ajoutées étaient de 5, 10 et 15% molaires. Trois voies ont été comparées: précipitation des hydroxydes à partir des nitrates dans l'ammoniaque sur la surface du Si_3N_4, précipitation en l'absence de Si_3N_4 suivie d'un mélange mécanique et homogénéisation des oxydes et du Si_3N_4 dans un broyeur par attrition. Nous avons constaté que la calcination des poudres était une étape critique en raison du risque d'oxydation qui entraîne la formation de Si_2N_2O et ralentit la densification. La poudre précipitée calcinée à 900°C sous azote atteint, dans des conditions de frittage identiques, une densité supérieure de 2·7% à celle des autres poudres.

1 Introduction

Si_3N_4 ceramics were successfully tested as structural components in service under mechanical, thermal and corrosive loads.[1] The manufacturing of dense

Journal of the European Ceramic Society 0955-2219/90/$3.50

ceramic bodies requires the addition of oxides which react with the oxygen surface layer of Si_3N_4 to form a high temperature melt. This melt promotes densification and is a necessary requirement for pressureless sintering of Si_3N_4.[2,3] The melt undergoes glass transition on cooling and is visible as a glassy phase between the grains in the microstructure.[4,5] The glassy phase is necessary for sintering but it also determines the high temperature mechanical properties in a detrimental way. The strength of a Si_3N_4 body is limited up to the temperature when the glassy phase melts and allows creep rupture, since the glassy phase allows grain boundary shearing and promotes creep of the bodies.[6] The glassy phase is additionally a fast diffusion path and enhances the oxygen diffusivity leading to lower oxidation resistance.[7,8] The ambivalent effects of the glassy phase have created the desire to reduce the amount of glassy phase, i.e. the amount of additives.

The aim of this work was to reach a higher geometrical and chemical homogeneity of the additives within the powders. Analogous to the development of oxide powders only a wet chemical preparation route can give a sufficiently small crystallite size and suitable chemical homogeneity. In general, there are various routes in wet chemical preparations, such as salt precipitation,[9,10] spray reacting,[11] hydrothermal treatments,[12] alkoxide hydrolysis[13,14] and different polymer routes.[15,16] For this work the precipitation of nitrate solution with stoichiometric quantities of the chosen cations into concentrated ammonia was used. Similar precipitation routes were intensively investigated for the ZrO_2 precipitation. The advantage of this process is the low price of the salt precursor and the possibility to scale up such a process. Three different routes

—coprecipitation and subsequent mixing (SP),
—coprecipitation in the presence of Si_3N_4 (CP),
—mechanical mixing by an attrition (MM).

were compared. The different routes will be hereforth referred by these abbreviations.

2 Experimental Procedure

Three kinds of Si_3N_4 (LC12, H. C. Starck, Berlin, FRG) mixtures with 5, 10 and 15 mol% YAG ($3Y_2O_3 . 5Al_2O_3$) were prepared by routes described in Fig. 1, whose details will be reported in the following subsections.

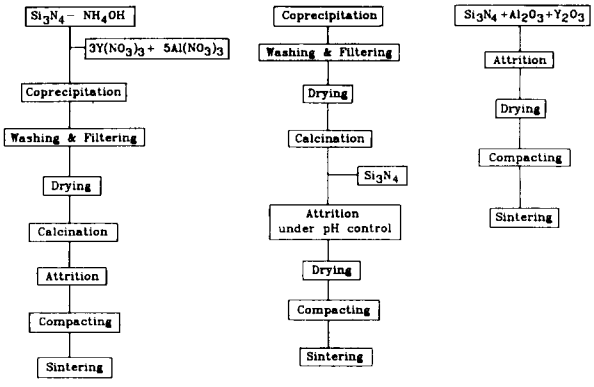

(a) CP (b) SP (c) MM

Fig. 1. Schematic diagram of preparation routes.

2.1 Coprecipitation of hydroxides in absence of Si_3N_4

For determination of optimal condition for preparation of homogeneous additives by coprecipitation, some experiments were carried out in absence of Si_3N_4. Primarily, titration curves for $Y(NO_3)_3$, $Al(NO_3)_3$ and their mixture with 3:5 molar ratio were obtained by NH_4OH addition. Concentrations of solutions used were 0·1 and 0·5M. Calcination behavior of coprecipitated hydroxides was investigated by DTA and TGA (STA409, Netzsch Gerätebau, Selb, FRG) for dried powder under a constant heating rate of 2°/min from room temperature to 1000°C. Drying was performed at 60°C for 1 day followed by holding at 130°C for 1·5 h in air.

2.2 Preparation of Si_3N_4 with additives by coprecipitation

Under the conditions obtained from the abovementioned experiments, Si_3N_4 powder mixtures with additives were prepared by direct coprecipitation of hydroxides on Si_3N_4 particles. A stoichiometric solution of $Y(NO_3)_3$ /$Al(NO_3)_3$ (3:5 molar ratio) was sprayed into a suspension of Si_3N_4 in NH_4OH, being stirred by mechanical agitation. After the completion of precipitation, the powder suspension was filtered to eliminate the NH_4NO_3 and washed with neutralized water and ethanol. The dried powder mixture was calcined at 700 and 900°C, respectively, for 1 h under various atmospheres (air, N_2 and Ar).

2.3 Conventional preparations

For comparison of effectiveness of the coprecipitation method with that of the conventional mechanical mixing, Si_3N_4 was ground with Y_2O_3 (H. C. Starck, Berlin, FRG) and Al_2O_3 (A-16G, Alcoa, Pittsburgh, PA) in an attrition mill for 4 h, using 2·6 mm diameter alumina balls and isopropanol.

Another powder mixture of Si_3N_4 with separately coprecipitated and calcined additives was prepared by attrition milling for 4 h in distilled water with pH control. An optimum pH range for the strongest attractive force between Si_3N_4 and YAG powders was obtained from zeta potential mueasurements (Zetasizer IIc, Malvern, Worcestershire, UK).

Powder size and its distrubution were controlled by varying the attrition time so that they had the same conditions. Powder mixtures were isostatically pressed into cylindrical form (14·5 mm diameter and 11·9 mm height) under 200 MPa. Green densities were measured by Archimedes principle. Sintering was performed in a dilatometer (Astro Industries Inc., CA, USA) or a graphite furnace (Gero, Neuhausen, FRG) at 1700 and 1800°C for 0·5 h under a 1·3 bar N_2 atmosphere. The heating rates were 50°/min up to 1000°C and 10°/min to the final sintering temperature. Linear shrinkage, weight loss and sintered density were measured after the sintering experiment. Observation of powder morphology and sintered microstructure was carried out by TEM (JeolCX, Japan) and SEM (Stereoscan S-200, Cambridge Instruments, UK). The phase content after calcination and sintering were identified by XRD (Seifert MZIV, Ahronsbörg, FRG) measurement with step speed of 2°/min.

3 Results and Discussion

3.1 Coprecipitation of hydroxides in the absence of Si_3N_4

As can be seen in Fig. 2, equivalent points for $Y(NO_3)_3$, $Al(NO_3)_3$ and $3Y(NO_3)_3/5Al(NO_3)_3$ with NH_4OH are 8, 6·8 and 8·7, respectively. It means that only above pH 9 can complete coprecipitation be expected. Therefore, a highly concentrated NH_4OH(6M ≈ pH 12) was used to retain the necessary pH during the procedures. Even if re-dissolution of aluminium hydroxides after precipitation at high pH was reported,[17,18] chemical analysis on the remaining supernatant revealed no trace of aluminium and yttrium ions.

Thermogravimetric analysis data (Fig. 3(a)) show that the main weight loss occurred over all the investigated temperature ranges during heating of the dried hydroxides. The difference in weight loss between the measured (31 wt%) and the theoretical value (27 wt%) for dehydration of hydroxides might result from incomplete drying. Near 900°C an endothermic peak was observed from the DTA curve (Fig. 3(b)). This seems to be attributed to crystallization of amorphous YAG phase. XRD investigation supports this explanation (Fig. 4(a)). Whereas the powder calcined at 800°C shows no crystalline phase, calcination at 900°C results in apparent crystallization of amorphous precipitates. The grade of crystallization increased with temperature. The

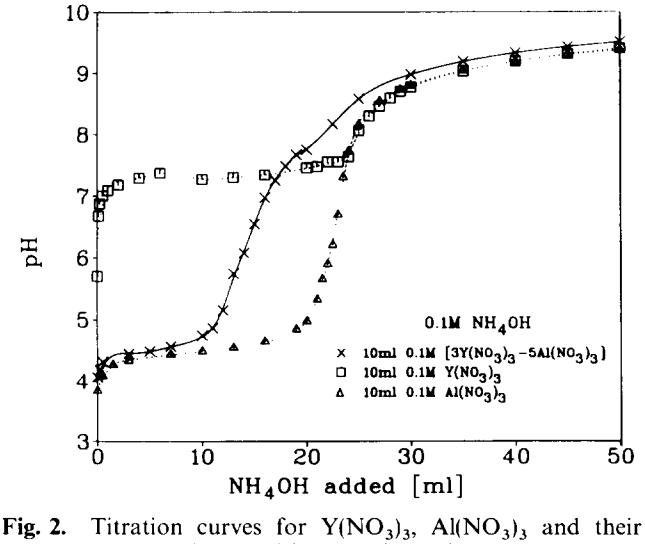

Fig. 2. Titration curves for $Y(NO_3)_3$, $Al(NO_3)_3$ and their mixture with 3·5 molar ratio.

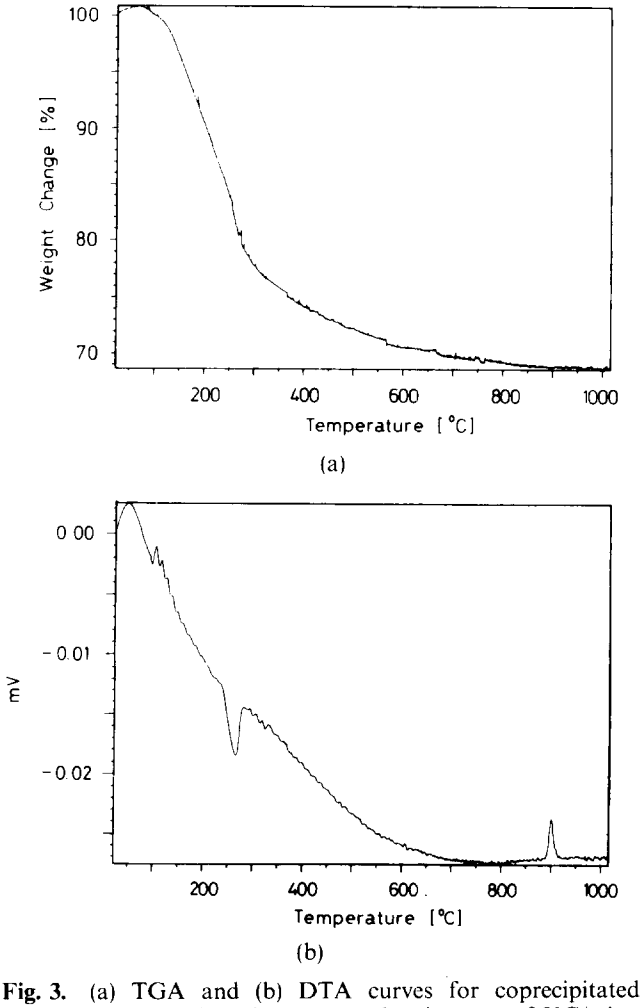

Fig. 3. (a) TGA and (b) DTA curves for coprecipitated hydroxide (3Y:5Al) under constant heating rate of 2°C/min.

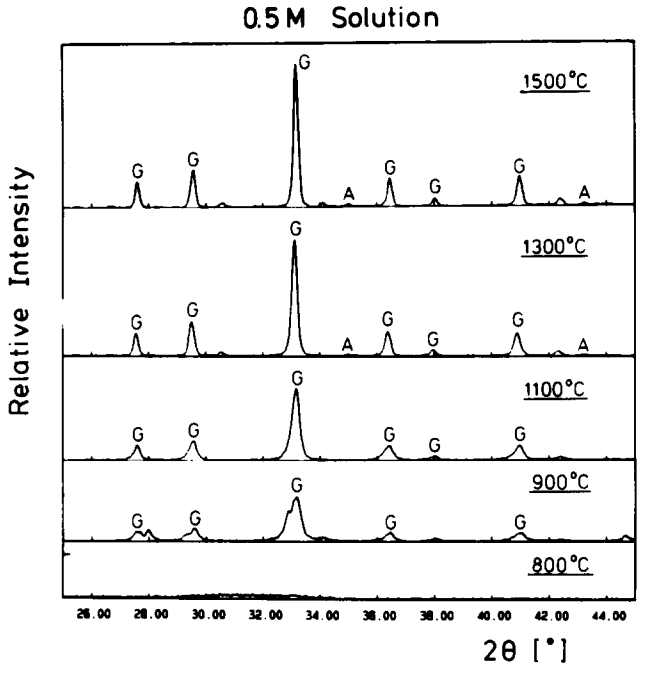

(a)

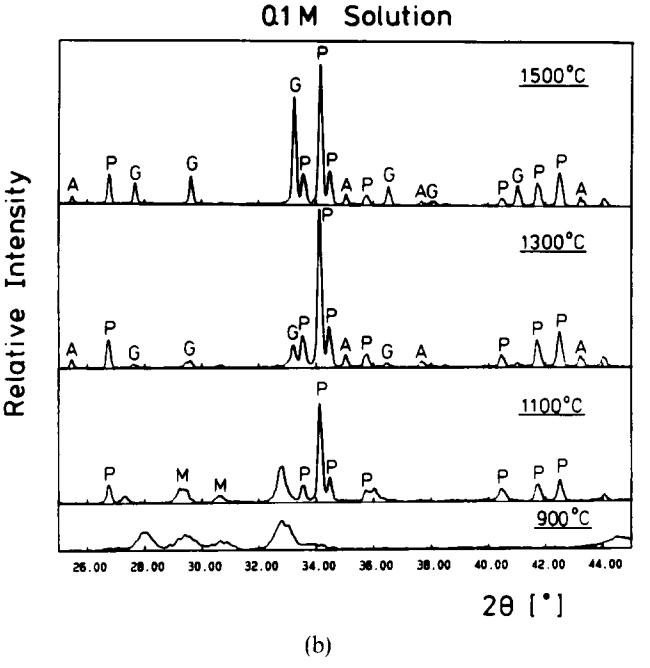

(b)

YAG phase is dominant, but a small amount of α-Al_2O_3 was detectable (marked A in Fig. 4(a)). For a lower concentration solution (Fig. 4(b)), the metastable YAM phase (2:1) was obtained besides a significantly larger amount of α-Al_2O_3 compared to Fig. 4(a). The reaction to the stable YAG phase is even more sluggish than the MM powder. A lower concentration of the solution results in a slower reaction rate, i.e. according to the titration curves, the aluminium hydroxide precipitates at a lower pH (see Fig. 2). The first crystalline phase will be an aluminum hydroxide or Al-rich Y-Al-hydroxide. According to the Al_2O_3–Y_2O_3 phase diagram (Fig. 5),

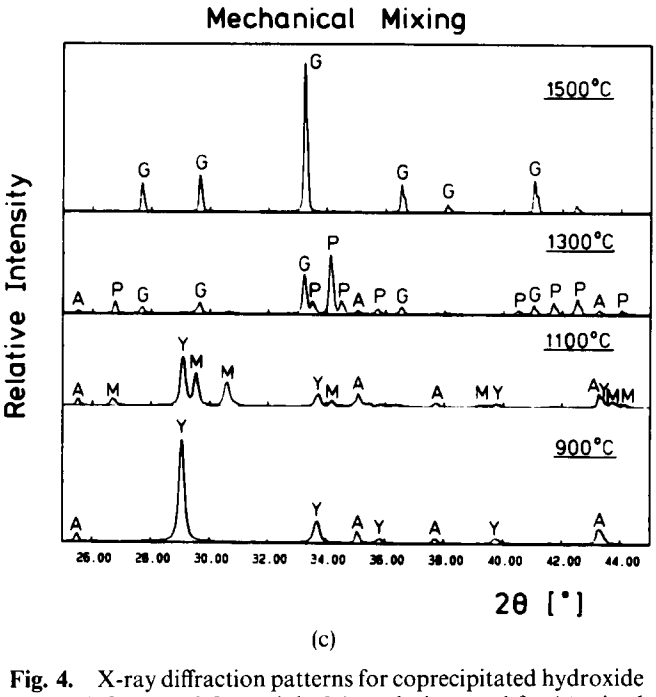

(c)

Fig. 4. X-ray diffraction patterns for coprecipitated hydroxide (3Y:5Al) from (a) 0·5M and (b) 0·1M solutions and for (c) mixed oxides after heat treatment at various temperatures (G:YAG (3:1), M:YAM(2:1), P:YAP(1:1), A:α-Al_2O_3 and Y:Y_2O_3).

α-Al_2O_3 and the YAM phase (2:1 phase) are primarily forming. Both are fairly stable substances and therefore the driving force for the YAG formation is considerably small even for the small sized crystallites. For highly concentrated solutions, the YAG forms directly with the exception of very low α-Al_2O_3 content. The higher reaction rate prevents most of the redissolution during the reaction, i.e. the powder is chemically almost

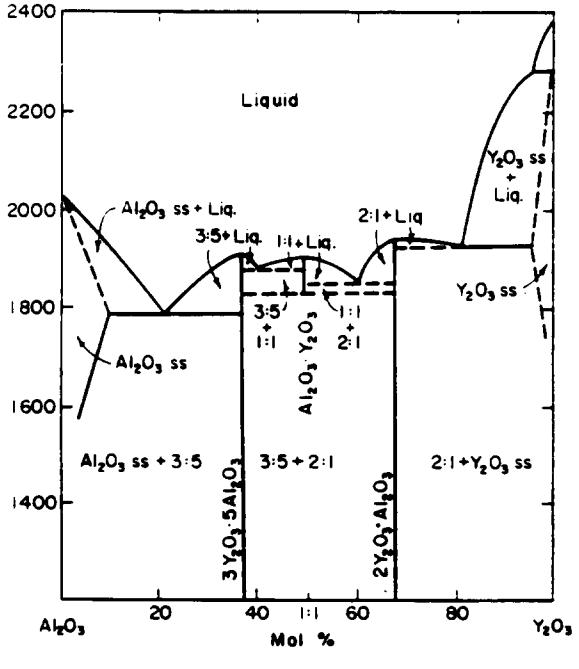

Fig. 5. Phase diagram of the Al_2O_3–Y_2O_3 system.

homogeneous and contains predominantly YAG. The particle size is about 30 nm in good agreement with that calculated from an X-ray broadening method, even if they are agglomerated due to their extremely fine particle size.

In contrast to the crystallization of a precipitated powder, the formation of a 3:5 phase of the mechanically mixed powder requires temperatures above 1300°C, hence, this reaction completed at temperature of 1500°C (Fig. 4(c)). This sluggish reaction is a consequence of the larger particle size (typically 0·3–0·5 μm for attrition-milled powder compared to ~30 nm crystallites of precipitated powder).

These results demonstrate the possibility that chemically homogeneous and extremely fine additive powders can be doped on Si_3N_4 particles by the coprecipitation method, since the surface of the Si_3N_4 particles would provide enough heterogeneous nucleation sites for the precipitates.

3.2 Preparation of Si_3N_4 with additives by coprecipitation

Under the conditions obtained from above results, Si_3N_4 powder was mixed with additives by the coprecipitation method. Figures 6(a–c) show the particle size distributions for powders after precipitation/drying, calcination and post-attrition, respectively. After precipitation/drying, Si_3N_4 particles formed very hard agglomerates with the cooperation of gellic precipitates (up to 30 μm). The proportion of large agglomerates was increased by further calination. These hard agglomerates must be destroyed, because they are known to be one reason for differential sintering. Such a local densification leads to retarding of shrinkage and formation of inhomogeneities and flaws, respectively, in the final microstructure. In fact, we could never obtain a sintered sample with higher than 90% TD from as-calcined powder, so, in any case a milling treatment was required. XRD investigations on coprecipitation-mixed Si_3N_4 powders show that in addition to the α and β phases of Si_3N_4 the crystallized YAG phase can be obtained after calcination at 900°C for 1 h regardless of atmosphere (air, N_2 and At), similar to the case of oxide coprecipitation. A TEM micrograph of this powder is given in Fig. 7. Extremely fine particles (< 50 nm) of precipitates are partly covering the large Si_3N_4 grains (mean size = 0·5 μm). However, a more careful observation of the figure shows that not all the surfaces of the Si_3N_4 grains were completely covered by precipitates. There are precipitates without any contact with the Si_3N_4 surfaces. The incomplete surface coating can result from an inadequate

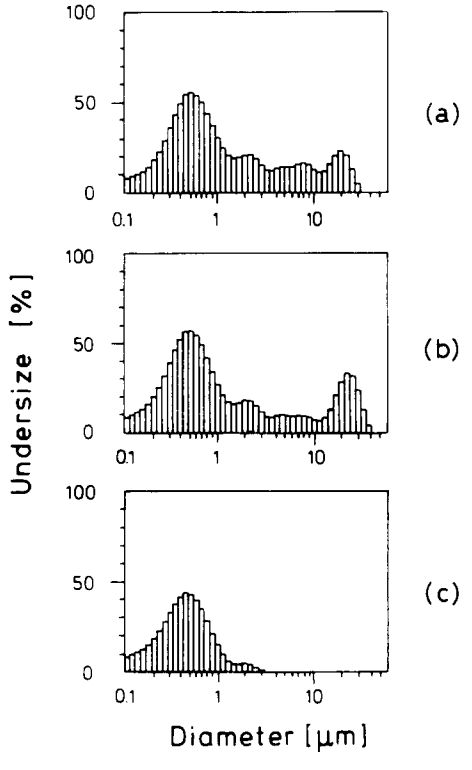

Fig. 6. Particle size distributions for Si_3N_4 with 10 mole % YAG after (a) coprecipitation/drying, (b) calcination ($T = 900$°C) and (c) post-attrition.

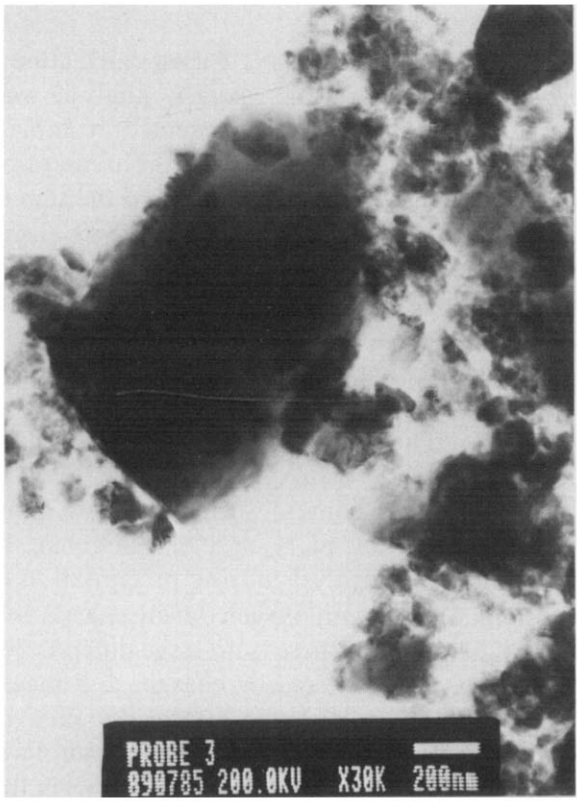

Fig. 7. TEM micrograph of Si_3N_4 with coprecipitated YAG-additive.

Table 1. Oxygen content for different charges of Si_3N_4 powder with 5 mol% YAG (wt%)

Charge	*Preparation procedure*	*Measured*	*Expected*	*Excess*
1	CP → C (Air:900°C) → NA	6·1	3·8	2·3
2	VA → CP → C(N_2:900°C) → NA	5·2	4·4	0·8
3	VA → CP → C (Ar:700°C)	4·2	4·2	0
4	SP → A (under pH control)	4·8	4·2	0·6
5	A (with oxides in isopropanol)	4·5	4·2	0·3

VA: pre-attrition; NA: post attrition; A: attrition; CP: co-precipitation; SP: separate precipitation; C: calcination.

precipitation technique. The first contact point of the salt solution and the ammonia is the surface of the suspensions and not necessarily the Si_3N_4 surface. Doped layers of precipitates could be destroyed by post-attrition. Besides the above-mentioned possibilities, another reason can be suggested from the point that a perfect coating requires a receptive Si_3N_4 surface. According to recent investigations on the surface character of Si_3N_4,[19–21] there are not only favorable silanol (SiOH) groups for precipitation of hydroxides but also silylamine ($SiNH_2$ or SiNH) groups, on which Y^{3+} and Al^{3+} ions cannot be adsorbed. The surface modification of Si_3N_4 might improve the quality of the additive coating. In this work, however, Si_3N_4 has been used without any modification and the preparation of a receptive surface must be left for future work.

3.3 Surface oxidation of Si_3N_4 during calcination

After powder preparation, oxygen analysis was performed, and the results are presented in Table 1 for Si_3N_4 with 5 mol% YAG. Under the assumption that total oxygen content is composed of the sum of proportion from the intrinsic existing SiO_2 layer on the surface of the Si_3N_4 particles (2 wt% O_2), additive oxides (1·7 wt% O_2) and contamination by Al_2O_3 balls during attrition (0·1–0·7 wt% O_2 depending on the attrition time), the expected oxygen content after preparation should be calculated as 3·8–4·4 wt %. The measured values indicate an additional pick-up of oxygen up to 2·3 wt %. Increase in oxygen content seems to result from surface oxidation of Si_3N_4,[22–24] which can be caused either by hydrolysis during precipitation or by reaction of Si_3N_4 with oxygen during calcination. However, the fact that there is no large difference in the excess oxygen content for charges 2–5 means that the oxidation due to hydrolysis can be considered as insignificant, because isopropanol was used in charge 5 and consequently hydrolysis in this charge was nearly impossible. As can be seen in the table, calcination in air at 900°C brought the largest increase in oxygen content. If such an increase in oxygen was related only to the formation of SiO_2 on Si_3N_4, it accounts for 4·3 wt % SiO_2 excess. This excess SiO_2 reacts with Si_3N_4 in the presence of the liquid phase during heating and forms crystalline Si_2N_2O,[25] which affects sintering behavior negatively by increasing the viscosity of the liquid phase. Figure 8 demonstrates the role of excess oxygen content on the sintering behavior of Si_3N_4. The upper curve in Fig. 8(a) shows the densification of Si_3N_4 calcined in N_2 with only 0·8 wt% excess oxygen (charge 2 in Table 1). The final density of 96·5% TD had already been reached during the

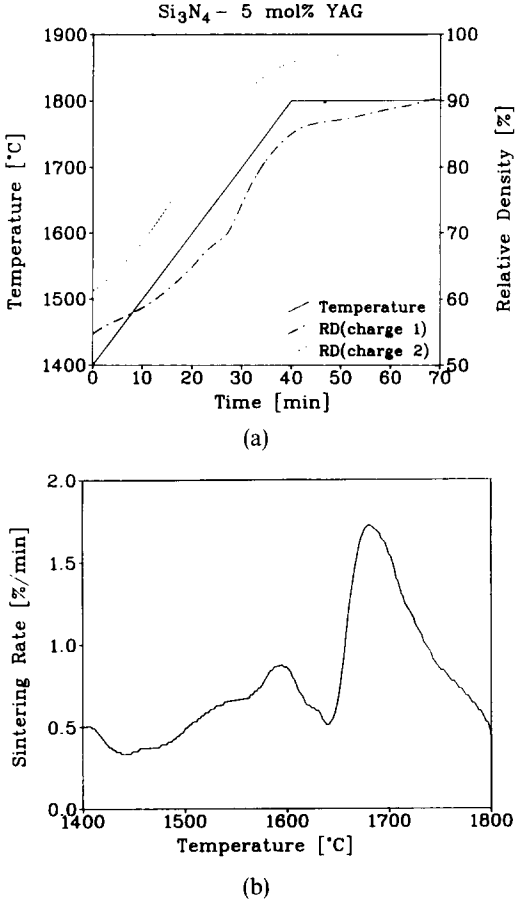

Fig. 8. (a) Sintering curve for Si_3N_4 with 5 mole % YAG sintered at 1800°C for 30 min and (b) change in sintering rate as a function of temperature.

heating stage. The lower curve shows the retarded densification of a sample with 2·3 wt % excess oxygen (charge 1). A significant drop in the densification rate was observed at 1640°C (Fig. 8(b)). Besides the α and β phases of Si_3N_4, a Si_2N_2O phase was identified for these specimens (Fig. 9). It has to be mentioned that, even if small amounts of Si_2N_2O phase were observed for all the 5 mole % samples, the relative peak intensities of the β-Si_3N_4 (210) to the Si_2N_2O (021) show that its content in the samples calcined in N_2 ($I_{SN(210)}/I_{SNO(021)} = 30{\cdot}1{:}1$) is smaller than in the samples calcined in air (7·75:1). For samples with 10 or 15 mole %, respectively, the Si_2N_2O phase appeared only in air calcined batches. After Greil *et al.*,[25] SiO_2 and Si_2N_2O form a eutectic composition at 1590°C, above which the formation of new liquid phase can start (see Fig. 10). It can be thought that this liquid phase again enhances the sintering rate above 1640°C.

A difference in temperature of 50°C may result from incomplete equilibrium due to the relatively high heating rate (10°/min), because no difference was obtained in another sintering experiment with 4°/min heating rate. Since over 1750°C at 1 atm gradual decomposition of Si_2N_2O takes place, acceleration of densification ceased with a further increase in temperature. Such a decomposition was well related to high weight loss in oxygen-riched specimens (7·5%), compared to that of specimens calcined in N_2 (2·1%).

The calcination was found to be a key step in the preparation of the powder. There is a risk of oxygen contamination which would make a short calcination cycles favourably, but, on the other hand, there is also a risk of incomplete reaction especially for larger batches. For this work calcination of 50 g batches in N_2 were found to have an acceptable compromise.

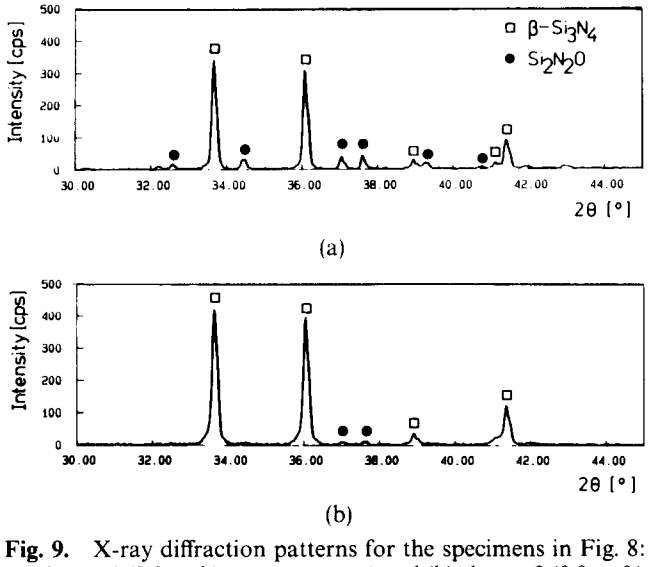

Fig. 9. X-ray diffraction patterns for the specimens in Fig. 8: (a) charge 1 (2·3 wt % excess oxygen) and (b) charge 2 (0·8 wt % excess oxygen).

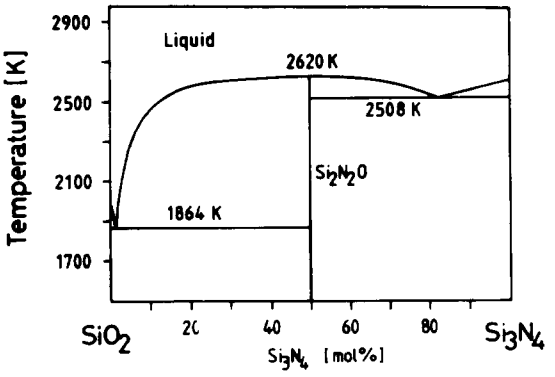

Fig. 10. The calculated system SiO_2–Si_3N_4 (after Ref. 25).

3.4 Sintered densities

The change in linear shrinkage of specimens with 5 and 10 mole % YAG was described as a function of sintering temperature in Fig. 11. All specimens were held at sintering temperature for 30 min. Irrespective of additive content and temperature, CP powder compact shows a higher shrinkage than MM powder. For 10 mole % additive content, both MM and CP powders reached their final density at 1600°C. For 5 mole % additive content, however, a continuous increase in shrinkage with temperature was observed. This effect was stronger for CP powders. From X-ray analysis, it can be concluded that an amount of only 12–21% β-Si_3N_4 was transformed up to 1600°C, depending on additive content. As the temperature was increased to 1700°C, the β-content increased to 50 and 70% for 5 and 10 mole % YAG, respectively. The reprecipitation of β-Si_3N_4 began in the temperature range between 1600 and 1700°C. Newly formed β-grains

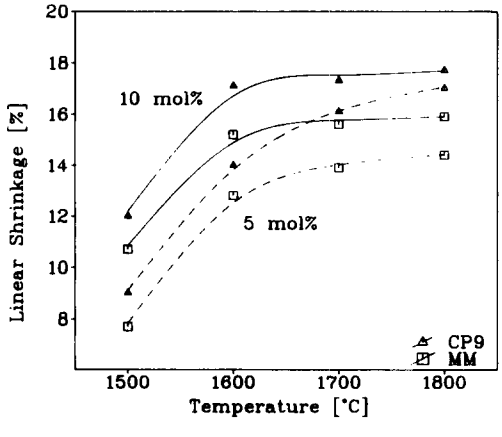

Fig. 11. Change in linear shrinkage of Si_3N_4 with 5 and 10 mole % YAG added by CP and MM as a function of sintering temperature (soaking time = 30 min).

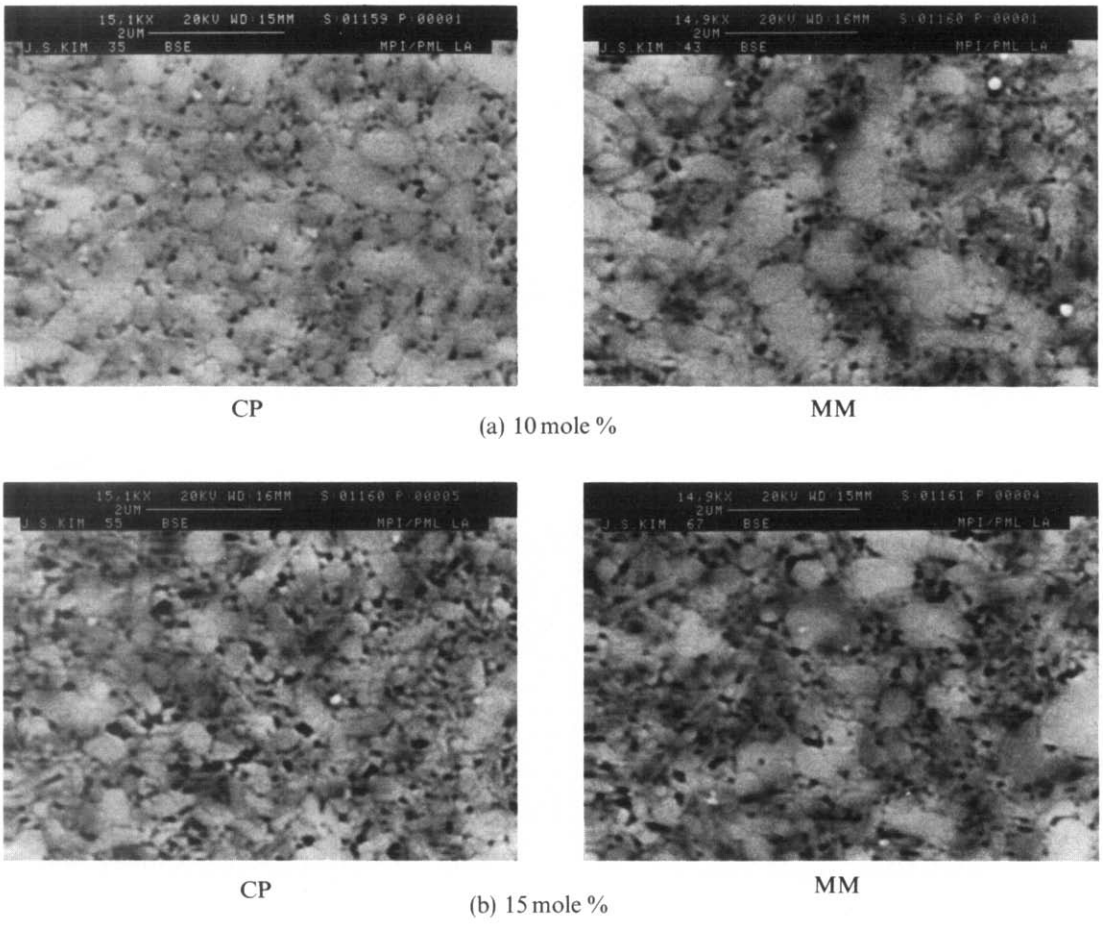

Fig. 12. Sintered microstructures of Si_3N_4 with (a) 10 and (b) 15 mole % YAG added by CP and MM (1700°C, 30 min).

had a very fine needle-like shape (about 0·5 μm for 15 mole % YAG specimen at 1700°C) (Fig. 12). Increasing the temperature to over 1700°C resulted in rapid grain growth and anchoring of β grains, which seems to hinder further densification.

Figures 13 (a)–(b) show relative densities as a function of mixing method for specimen with 5 and 10 mole % YAG sintered at 1700 and 1800°C for 30 min. In 5 mole % specimens, CP powder has the highest sintered density of 96·5% theoretical density in comparison with 93·8% for MM compact. There is no significant difference in sintered density for 10 mole % specimens relative to mixing methods, which is attributed to the good possibility of rearrangement in systems with a large amount of liquid phase.

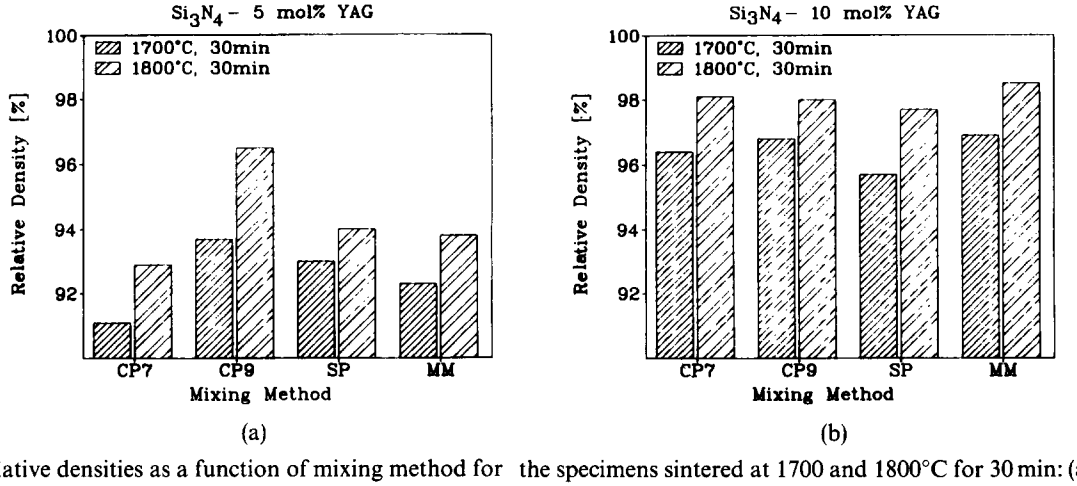

Fig. 13. Relative densities as a function of mixing method for the specimens sintered at 1700 and 1800°C for 30 min: (a) 5 and (b) 10 mole % YAG.

4 Conclusion

By means of the coprecipitation method the chemically homogeneous sintering additives (YAG) could be doped on Si_3N_4. Single phase YAG particles on Si_3N_4 were obtained after calcination at 900°C. The particles had a size <30 nm and were evenly distributed. Calcination in air caused an increase in oxygen content, which is related to the formation of new SiO_2 layers on Si_3N_4. Increased SiO_2 content resulted in retardation of densification and high weight loss by formation and decomposition of the Si_2N_2O phase during sintering.

The densification by shrinkage in 10 and 15 mole % YAG specimens seems to cease earlier than in 5 mole %. As a possible explanation, the fast transformation of α to β and grain growth of β-Si_3N_4 was suggested. Comparison of sintered densities for 5 mole % specimens showed apparent advantage in coprecipitation methods. In 10 and 15 mole % no considerable difference in density could be obtained. However, investigation of microstructures revealed more homogeneous and finer grains from the coprecipitation methods, irrespective of additive content.

References

1. Bunk, W., Böhmer, M. & Kissler, H., In *Keramische Komponenten für Fahrzeug-Gas-Turbinen III*, Springer Verlag, Berlin/Heidelberg, 1984.
2. Terwillinger, G. R. & Lange, F. F., *J. Mat. Sci.*, **10**(7) (1975) 1169–74.
3. Loehman, R. E. & Rowcliffe, D. J. *J. Am. Ceram. Soc.*, **63**(3–4) (1980) 144–8.
4. Clarke, D. R. & Thomas, G., *J. Am. Ceram. Soc.*, **60**(11–12) (1977) 491–5.
5. Greil, P. & Petzow, G., *Proc. Int. Symp. on Ceramic Components in Engines*, Hakone, Japan, 1983.
6. Clarke, D. R., *Progress in Nitrogen Ceramics*, ed. F. L. Riley, Martinus Nijhoff Publishers, The Hague, The Netherlands, 1983, pp. 341–58.
7. Lewis, M. H. & Barnard, P., *J. Mat. Sci.*, **15** (1980) 443–8.
8. Mieskowski, D. M. & Sanders, W. A., *J. Am. Ceram. Soc.*, **68**(7) (1985) C160–3.
9. Moyer, J. R., Prunier, A. R. Jr, Hughes, N. N. & Winterton, R. C., *Mat. Res. Soc. Symp. Proc.*, **73** (1986) 117–22.
10. Shaw, T. M. & Bethica, B. A., *J. Am. Ceram. Soc.*, **69**(2) (1986) 88–93.
11. Haug, T., *Symposium Material Forschung 1988*, Hamm, FRG, Federal Ministry of Science and Technology, FRG, 1988, p. 578.
12. Kriechbaum, G. W., Hartmann, W. & Peuckert, D., *Symposium Material Forschung 1988*, Hamm, FRG, Federal Ministry of Science and Technology, FRG, 1988, p. 592.
13. Mitomo, M., Shogai, T., Yoshimatsu, H. & Kotami, Y., *J. Ceram. Soc. Japan*, **93**(7) (1985) 364–9.
14. Kishi, K., Umebayashi, S., Pompe, R. & Persson, M., *J. Ceram. Soc. Japan*, **96**(6) (1988) 698–701.
15. Micheli, A. L., *Ceramics International*, **15** (1989) 131–9.
16. Schwartz, K. B., Rowcliffe, D. J. & Blum, Y. D., *Adv. Ceram. Mat.*, **3**(4) (1988) 320–3.
17. Archibald, E. H. & Habasian, Y., *P. Trans. Soc. Can.*, **11**(3) (1917) 4.
18. Ivanov-Emine, B. N., Niel'son, L. A. & Ivolgina, A. T., *Russ. J. Inorg. Chem.*, **6** (1961) 1483–4.
19. Stadelmann, H., Greil, P. & Petzow, G., *J. Euro. Ceram. Soc.*, **5** (1989) 155–63.
20. Whitmann, P. K. & Feke, D. L., *J. Am. Ceram. Soc.*, **71**(12) (1988) 1086–93.
21. Bergström, L. & Pugh, R. J., *J. Am. Ceram. Soc.*, **72**(1) (1989) 103–9.
22. Immamura, Y., Ishibashi, K. & Shimodairo, H., *Ceram. Engng Sci. Proc.*, **7** (1986) 828–38.
23. Rahaman, M. N., Boiteux, Y. & De Jonghe, L. C., *Am. Ceram. Soc. Bull.*, **65**(8) (1986) 1171–6.
24. Peuckert, M. & Greil, P., *J. Mat. Sci.*, **22** (1987) 717–20.
25. Dörner, P., Gauckler, L. J., Krieg, H., Lukas, H., Weiss, J. & Petzow, G., *J. Mat. Sci.*, **16** (1981) 935.
26. Huang, Z. K., Greil, P. & Petzow, G. *Ceramics International*, **10** (1984) 14–17.